Eur. Phys. J. B **62**, 459–464 (2008)
DOI: 10.1140/epjb/e2008-00194-9

THE EUROPEAN PHYSICAL JOURNAL B

Generalization of a nonlinear friction relation for a dimer sliding on a periodic substrate

M. Tiwari[1,a], S. Gonçalves[2], and V.M. Kenkre[1]

[1] Consortium of the Americas for Interdisciplinary Science and Department of Physics and Astronomy, University of New Mexico, Albuquerque, New Mexico 87131, USA
[2] Instituto de Física, Universidade Federal do Rio Grande do Sul, Caixa Postal 15051, 91501-970 Porto Alegre RS, Brazil

Received 19 February 2008 / Received in final form 6 April 2008
Published online 22 May 2008 –

Abstract. An atomic cluster moving along a solid surface can undergo dissipation of its translational energy through a direct mode, involving the coupling of the center-of-mass motion to thermal excitations of the substrate, and an indirect mode, due to damping of the internal motion of the cluster, to which the center-of-mass motion can be coupled as a result of surface potential. Focussing only on the less well understood indirect mode, on the basis of numerical solutions, we present, departures from a recently reported simple relationship between the force and velocity of nonlinear friction. A generalization of the analytic considerations that earlier led to that relationship is carried out and shown to explain the departures satisfactorily. Our generalization treats for the system considered (dimer sliding over a periodic substrate) the complete dependence on several of the key parameters, specifically internal dissipation, natural frequency, substrate corrugation, and length ratio. Further predictions from our generalizations are found to agree with new simulations. The system analyzed is relevant to nanostructures moving over crystal surfaces.

PACS. 81.40.Pq Friction, lubrication, and wear – 46.55.+d Tribology and mechanical contacts

1 Introduction

The friction experienced by atoms, small molecules and adlayers moving on substrates is an active topic of current research [1–7,16] because of its relevance to the fundamental understanding of a variety of processes such as those involved in atomic force microscopy [8,9]. Taking the natural point of view that a thorough understanding of the motion of idealized atomic structures over idealized substrates should precede the study of the motion of realistic atomic entities over realistic surfaces, several investigators have explored the motion of dimers (two-atom systems) moving over a fixed surface represented by a sinusoidal [10–15] potential. It is perhaps surprising but true that, in spite of the fact that a number of thorough studies of more realistic (e.g., extended) systems have already appeared in the literature, interesting results continue to be found in the simple dimer system. If a dimer characterized by the mass m of each atom connected by a spring of spring constant $m\omega_0^2$ is thrown with an initial center of mass velocity v_0 over a 1-dimensional substrate represented by a sinusoidal potential of amplitude u_0 and wavelength b, one of these recent numerical investigations [10] showed that, if the only damping in the system acts on the *internal* coordinate of the dimer, the center of mass motion of the dimer is effectively damped in a remarkable fashion represented by a nonlinear friction relation. That relation states that the effective friction force experienced by the dimer center of mass motion is inversely proportional to the cube of the center of mass velocity. The purpose of the present paper is to investigate the range of validity of that friction relation. We carry out numerical simulations that go beyond the limiting set of conditions explored in reference [10], show that clear departures are obtained in the behavior of the dimer including in the dependence of its stopping time on various system parameters, and provide a satisfactory theoretical explanation for our findings.

The paper is set out as follows. We first investigate numerically the departures from the simple nonlinear friction relation of reference [10] with change in system parameters (Sect. 2) and then give a simple explanation in terms of an extended nonlinear friction relation to support our numerical findings (Sect. 3). In Section 4 we make predictions on the basis of our analysis and find that they are verified by new numerical solutions. Concluding remarks are presented in Section 5.

2 Departures from the $1/v^3$ friction relation

The equations of motion governing the system under study, a dimer moving on a 1-dimensional periodic

[a] e-mail: mukesh@unm.edu

substrate, are

$$\begin{aligned} m\ddot{x}_1 = \; & k(x_2 - x_1 - a) + \left(\tfrac{2\pi u_0}{b}\right) \sin\left(\tfrac{2\pi x_1}{b}\right) \\ & -\tfrac{m\gamma}{2}(\dot{x}_1 - \dot{x}_2) \\ m\ddot{x}_2 = \; & -k(x_2 - x_1 - a) + \left(\tfrac{2\pi u_0}{b}\right) \sin\left(\tfrac{2\pi x_2}{b}\right) \\ & -\tfrac{m\gamma}{2}(\dot{x}_2 - \dot{x}_1) \end{aligned} \quad (1)$$

where $x_{1,2}$ are the coordinates of the two dimer particles of equal mass m, overdots denote time derivatives, γ is the damping coefficient and k, a, b, u_0 are, respectively, the spring constant, equilibrium length of the dimer, wavelength of the substrate potential and half the amplitude of the potential. Note that the damping of each mass is proportional not to its absolute velocity but to the velocity relative to the other mass. This means that damping acts *only* on the internal coordinate. Such a situation represents dissipation of energy through channels internal to the moving structure. We consider the system at temperatures low enough that random (Brownian motion) terms need not be added in equation (1). This we do for simplicity as in reference [10]. It has been pointed out in various papers such as reference [11] how the Brownian terms may be incorporated.

The authors of reference [10] have shown, through simulations and analytic indications starting from equation (1), that the dimer dynamics can result in the remarkably simple nonlinear friction relation:

$$\frac{dv}{dt} = -\frac{\gamma}{2}\left(\frac{u_0}{m}\right)^2 \sin^2\left(\frac{\pi a}{b}\right)\frac{1}{v^3}. \quad (2)$$

Equation (2) predicts that the stopping time (defined as the time at which the velocity of the center of mass drops to zero) would be given as:

$$t_s = \frac{v_0^4}{2\gamma\left(\frac{u_0}{m}\right)^2 \sin^2\left(\frac{\pi a}{b}\right)}. \quad (3)$$

This means that the stopping time for the center of mass motion should vary inversely as the coefficient γ which controls the damping in the internal coordinate of the dimer.

The first of the departures from the friction relation given by equation (2) that we report in the present paper is the *violation of the monotonic* γ-dependence of the stopping time. We plot in Figure 1 the variation, with change in the damping coefficient γ, of the stopping time obtained by solving numerically equation (1). The plot clearly shows that departure. The solution we obtain (solid curve) coincides with the prediction of equations (2, 3) initially, showing a decrease in t_{stop} with increasing γ. However, further increase in γ results in an *increase* in t_{stop}, in contrast to the predictions of equations (2, 3). In examining the dependence of t_{stop} on γ, we have found a striking linear relationship between γ^2 and the relative difference between t_{stop} and the stopping time t_s predicted by the $1/v^3$ relation set out in reference [10]. We exhibit this linear relationship in Figure 2.

The second departure from predictions of the relation in equations (2, 3) that we found involves the *frequency-dependence* of the stopping time. While equation (2) is

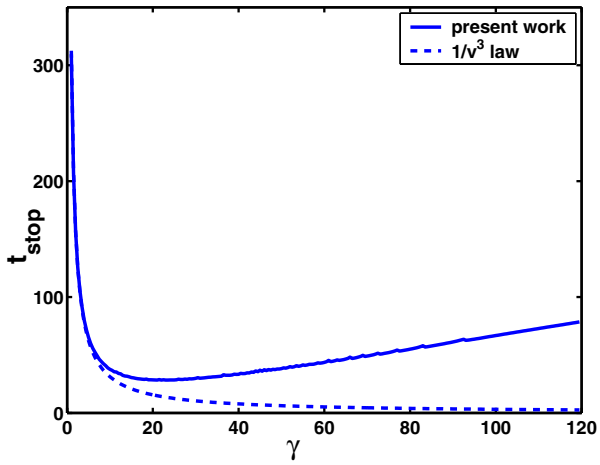

Fig. 1. Departure from the friction relation of reference [10]: comparison between the non-monotonic stopping time t_{stop} obtained from numerical simulations (solid line) with the monotonic prediction (see Eq. (3)) of the $1/v^3$ relation (dashed line) of reference [10] for different values γ of damping. Damping is expressed in units of $(1/b)\sqrt{u_0/m}$ and stopping time is in units of $b\sqrt{m/u_0}$. Initial velocity v_0 is $5\sqrt{u_0/m}$. Other parameters are $a/b = 0.5$ and $kb^2/u_0 = 0.02$.

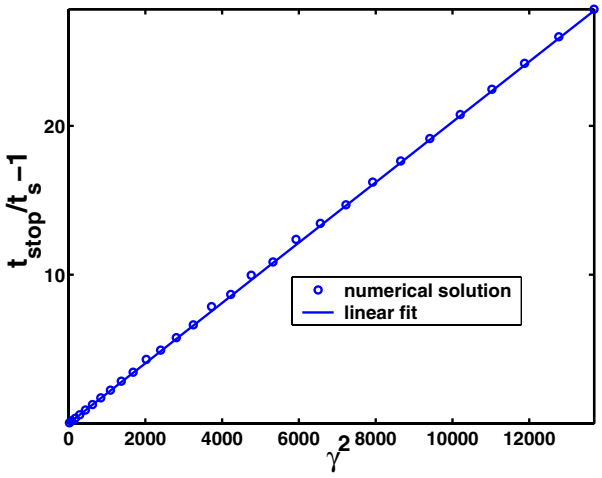

Fig. 2. Linear relationship between γ^2 and the relative difference between the stopping time and the prediction of the friction relation in reference [10]. The circles represents the numerical solution while the solid line is an (excellent) linear fit. Other parameters are as in Figure 1.

independent of the natural frequency $\omega_0 = \sqrt{2k/m}$ of the dimer, our numerical solutions show that t_{stop} does exhibit a dependence on ω_0, showing a minimum and increase on either side of the minimum. We display this behavior in Figure 3, where we plot t_{stop} normalized to its limit t_0 as $\omega_0 \to 0$. The marked oscillatory behavior to the left of the minimum in Figure 3 is representative of the resonance as will be clear from Figure 4 below. The rest of the jagged nature of the curve in Figure 3 has no physical significance and arises from numerical sources.

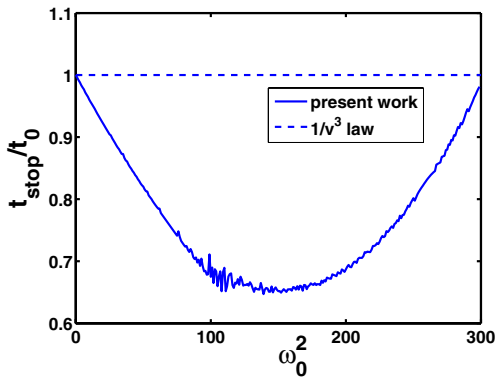

Fig. 3. Departure from the friction relation of reference [10] as seen in the dependence of the stopping time on the dimer natural frequency ω_0. Shown is the stopping time (normalized to its value t_0 for $\omega_0 \to 0$, see text) from our numerical solutions (solid line) and from the prediction of equations (2, 3) (dashed line), i.e., of the earlier analysis reference [10]. Frequency is expressed in units of $(1/b)\sqrt{u_0/m}$ and $\gamma b\sqrt{(m/u_0)} = 1$. Other parameters are as in Figures 1, 2.

3 Analytic studies from an extended version of the friction relation

In order to understand the source of the departures from the $1/v^3$ relation reported in Section 2, we examine the equations of motion (1) by following the procedure set out in reference [10]. By defining a scaled and translated coordinate ξ, through

$$\xi = \frac{(x_2 - x_1)}{a} - 1, \tag{4}$$

we obtain the equation of motion given in reference [10],

$$\frac{d^2\xi}{dt^2} + \gamma\frac{d\xi}{dt} + \omega_0^2\xi = \frac{4\pi u_0}{amb}\sin\left\{\frac{\pi a}{b}(1+\xi)\right\}\cos(\zeta), \tag{5}$$

where ζ, the scaled center of mass coordinate

$$\zeta = \frac{\pi(x_1 + x_2)}{b}, \tag{6}$$

obeys

$$\frac{d^2\zeta}{dt^2} = \left[\left(\frac{2\pi}{b}\right)^2\left(\frac{u_0}{m}\right)\right]\cos\left\{\frac{\pi a}{b}(1+\xi)\right\}\sin(\zeta)\cdot \tag{7}$$

It was argued in reference [10] that, although equation (7) predicts an involved dependence of ζ on ξ and, therefore, eventually on t, the simple linear approximation $\zeta(t)\approx\omega_a t$ where $\omega_a = 2\pi v(t)/b$ is the so called "washboard" frequency, $v(t)$ being the velocity of the center of mass, leads, for small ξ ($\xi \ll 1$), to

$$\frac{d^2\xi}{dt^2} + \gamma\frac{d\xi}{dt} + \omega_0^2\xi = \frac{4\pi u_0}{amb}\sin\left(\frac{\pi a}{b}\right)\cos(\omega_a t)\cdot \tag{8}$$

With equation (8) as the starting point, approximating the assumed weakly t-dependent ω_a to be a constant, one can solve for the internal coordinate

$$\xi(t) = \frac{4\pi u_0}{amb}\sin\left(\frac{\pi a}{b}\right)\frac{1}{\sqrt{\left(\omega_0^2 - \omega_a^2\right)^2 + \omega_a^2\gamma^2}}\cos(\omega_a t - \delta) \tag{9}$$

where δ is the phase angle given by $\tan(\delta) = \gamma\omega_a/(\omega_0^2 - \omega_a^2)$. The authors of reference [10] derived the nonlinear friction law by using a power balance condition. To be able to address the departures reported by us in Figures 1–3 above, we introduce an important modification in that argument. Instead of neglecting ω_0 and γ terms in

$$\frac{dv}{dt} = -\frac{\gamma}{2}\left(\frac{u_0}{m}\right)^2\sin^2\left(\frac{\pi a}{b}\right)\frac{v}{\left[v^2 - \left(\frac{b\omega_0}{2\pi}\right)^2\right]^2 + \left(\frac{b\gamma}{2\pi}\right)^2 v^2}, \tag{10}$$

we elect to use equation (10) as our generalized friction relation. Clearly, under the approximation that the washboard frequency ω_a is much larger than both the natural frequency ω_0 and damping γ, one gets the $1/v^3$ relation of reference [10]. Instead of simplifying equation (10) for $v \gg b\omega_0/2\pi$ and $v \gg b\gamma/2\pi$, we *solve* equation (10) exactly:

$$t = \frac{v_0^4}{4\eta}\left[\left\{1 - \left(\frac{v}{v_0}\right)^4\right\} + \left(\frac{b}{\pi}\right)^2\left(\frac{\gamma^2}{2v_0^2} - \frac{\omega_0^2}{v_0^2}\right)\left\{1 - \left(\frac{v}{v_0}\right)^2\right\} - \left(\frac{b\omega_0}{\sqrt{2}\pi v_0}\right)^4\ln\left(\frac{v}{v_0}\right)\right] \tag{11}$$

where, $\eta = \frac{\gamma}{2}\left(\frac{u_0}{m}\right)^2\sin^2\left(\frac{\pi a}{b}\right)$. The definition of the frequency $\omega = 2\pi v_0/b$, which is the *initial* value of ω_a, and corresponds to the initial center of mass velocity of the dimer, allows us to rewrite our solution (11) as

$$\frac{t}{t_s} = \left[1 - \left(\frac{v}{v_0}\right)^4\right] + 4\left(\frac{\gamma^2}{2\omega^2} - \frac{\omega_0^2}{\omega^2}\right)\left[1 - \left(\frac{v}{v_0}\right)^2\right] - 4\left(\frac{\omega_0}{\omega}\right)^4\ln\left(\frac{v}{v_0}\right) \tag{12}$$

where $t_s = \frac{v_0^4}{4\eta}$. Equation (12) is one of the principal analytic results of the present paper.

3.1 Analysis of the γ dependence of the stopping time for small internal frequency ($\omega_0 \ll \omega$)

The idea of putting $v = 0$ in equation (12), and calculating the corresponding stopping time t_{stop}, naturally suggests itself. However, it is not valid in general: the existence of the logarithmic term ensures that the velocity has a long-time tail which means that the stopping time is, strictly, always infinite. On the other hand, the simulations do show a stopping time within which the dimer falls into one of the substrate wells, and then rattles back and forth. A good estimate of t_{stop} can be obtained from equation (12) for values of ω_0/ω sufficiently small that the logarithmic

term can be neglected. Then, if the internal vibration frequency is small enough ($\omega_0 \ll \omega$), but if specifically we allow the damping γ to be unrestricted, we obtain

$$\frac{t}{t_s} = \left[1 - \left(\frac{v}{v_0}\right)^4\right] + \frac{2\gamma^2}{\omega^2}\left[1 - \left(\frac{v}{v_0}\right)^2\right]. \quad (13)$$

Putting $v = 0$ in equation (13), we get the stopping time

$$t_{stop} = t_s\left[1 + 2\left(\frac{\gamma}{\omega}\right)^2\right]. \quad (14)$$

Equation (14), another of the new results of the present analysis, displays the stopping time t_{stop} as the product of two factors. The first factor is the stopping time $t_s = \frac{v_0^4}{4\eta}$ given by the $1/v^3$ relation of reference [10]. The second factor is the correction provided by our present analysis: $1 + 2(\gamma/\omega)^2$. If damping is relatively small, which was the case treated earlier, $(\gamma/\omega)^2$ may be neglected and there is negligible correction. If, however, damping is substantial, t_{stop} as given by equation (14) can *increase* with γ. Indeed, (14) leads to

$$\frac{t_{stop}}{t_s} - 1 = \frac{2\gamma^2}{\omega^2}. \quad (15)$$

Our *analytic* result (15) provides the highly accurate fit to the simulations displayed in Figure 2.

3.2 Analysis of the ω_0 dependence of the stopping time for small damping ($\gamma \ll \omega$)

If, in equation (12), we make the approximation that the damping in internal coordinate is small ($\gamma \ll \omega$), but allow the frequency ω_0 to be unrestricted, we obtain

$$\frac{t}{t_s} = \left[1 - \left(\frac{v}{v_0}\right)^4\right] - \left(\frac{2\omega_0}{\omega}\right)^2\left[1 - \left(\frac{v}{v_0}\right)^2\right] - 4\left(\frac{\omega_0}{\omega}\right)^4 \ln\left(\frac{v}{v_0}\right). \quad (16)$$

Unlike in equation (14) we cannot obtain t_{stop} in this case by putting $v = 0$ in equation (16), because, as explained above, the stopping time is always infinite. To get an estimate of t_{stop} from (16), we put v/v_0 equal to a sufficiently small non-zero value c and solve (16) numerically. We call the stopping time thus obtained t'_{stop} rather than t_{stop} (because $c \neq 0$, although small) and display its dependence on the oscillator frequency in Figure 4. The value of c we have taken is obtained by equating the center of mass kinetic energy to the substrate potential energy.

The significant feature in the above case is the development of long tails of $v(t)$ that arise from the logarithmic term in the right hand side of (16). In the low-velocity limit ($v \ll b\omega_0/2\pi$) the denominator of the right hand side of equation (10) becomes independent of v and we recover the linear friction relation.

$$\frac{dv}{dt} = -\frac{\gamma}{2}\left(\frac{u_0}{mv_s^2}\right)^2 \sin^2\left(\frac{\pi a}{b}\right) v, \quad (17)$$

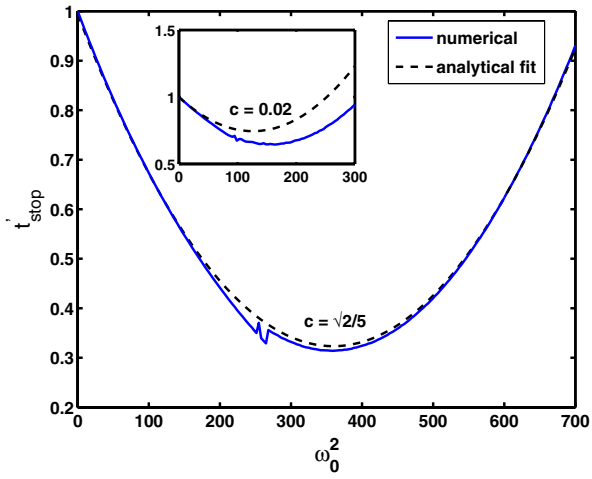

Fig. 4. Dependence of the apparent stopping time t'_{stop} on the oscillator frequency ω_0 showing close agreement between the numerical (solid line) and analytic expression given by equation (16) (dashed line) as explained, for different values of the natural frequency of the oscillator. The ratio c (see text) is taken to be $\sqrt{2}/5$. Frequency is expressed in units of $\sqrt{(u_0/m)}/b$ and $\gamma b\sqrt{(m/u_0)} = 1$. Other parameters are the same as in Figure 1. Inset shows the comparison for a smaller value of $c = 0.02$ which shows poor agreement of simulation and theory.

where, $v_s = \frac{b\omega_0}{2\pi}$ is the sliding velocity corresponding to the natural frequency of the oscillator. By fixing $v/v_0 = c$ and putting $dt/d\omega_0 = 0$ in our analytic equation (16), we can obtain a reasonable value of ω_0 at which the minimum of t_{stop} occurs in Figure 4: $\omega[(c^2-1)/2\ln c]^{-1/2}$.

This manner of getting stopping time would be completely useless if the results we obtain were strongly dependent on the chosen value of c. We have carried out numerous calculations for different c's and found that for $c \geq 0.2$ we get fine agreement between simulation and analytic prediction. For smaller values, we still find *qualitative* agreement (e.g. in the existence and approximate location of the minimum) which becomes worse as c is made smaller (see inset of Fig. 4). The oscillations seen to the left of the minimum occur when the driving frequency is close to resonance. This is obviously not present in our simple analytic results. The resonance is between the natural frequency of the dimer ω_0 and the washboard frequency $\omega_a = 2\pi v/b$ (see Eq. (9)).

4 Comparison of the predictions of the generalized friction relation with simulations

Given the satisfactory agreement of the analytic expression, equation (12), for the stopping time derived here, we present Figures 5, 6, where we compare the center of mass velocity according to our analytic expression (12) with numerical simulations. In Figure 5 we have kept the damping coefficient γ unchanged and have varied the natural frequency of the dimer to produce curves a, b, c from our analytic prediction for three different values of ω_0 as

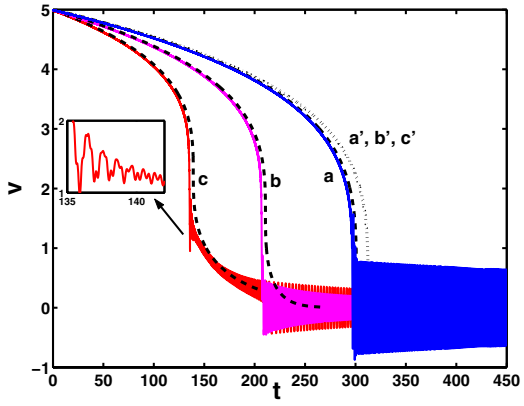

Fig. 5. Comparison between our present analytic prediction from the generalized friction relation (dashed lines) and numerical simulations (solid lines with oscillations) for the center of mass velocity $v(t)$. Initial velocity v_0 is $5\sqrt{u_0/m}$. Other parameters are $a/b = 0.5$ and $\gamma b\sqrt{m/u_0} = 1$. The different values of frequency ω_0 are 3.16, 10 and 14.14 expressed in units of $\sqrt{(u_0/m)}/b$. They correspond to the spring constant k being in the ratio 1:10:20 respectively. The lines a′, b′ and c′ are the predictions of the $1/v^3$ friction relation of reference [10] and coincide with one another because of the lack of appearance of the natural frequency in that relation. Velocity is expressed in units of $\sqrt{u_0/m}$ and time is in units of $b\sqrt{m/u_0}$. Inset shows the resonance structure that is visible in the main figure around $t = 140$.

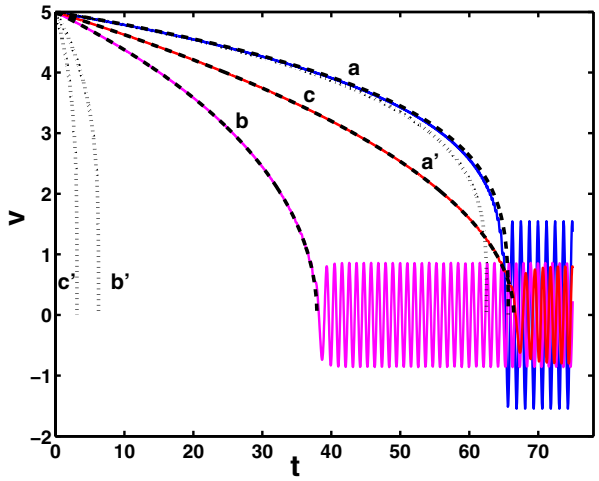

Fig. 6. Comparison between our present analytic prediction from the generalized friction relation (dashed lines) and numerical simulations (solid lines with oscillations) for the center of mass velocity $v(t)$ vs. time t. Initial velocity v_0 is $5\sqrt{u_0/m}$. Other parameters are $a/b = 0.5$ and $kb^2/u_0 = 0.02$. The different values of damping γ expressed in units of $\sqrt{(u_0/m)}/b$ are 5, 50 and 100. The dotted lines a′, b′ and c′ show the predictions of the $1/v^3$ friction relation. Velocity is expressed in units of $\sqrt{u_0/m}$ and time is in units of $b\sqrt{m/u_0}$.

shown. Our predicted curves sit right onto the simulation results until the latter break into oscillations which our analytic predictions cannot describe. Clearly, our present analysis does considerably better "vis-a-vis" the simulations than the $1/v^3$ relation which, being insensitive to ω_0, produces the *single* curve denoted a′, b′, c′ in Figure 5. The other feature our present simulations show is the resonance phenomenon when the washboard frequency equals the natural frequency. It is responsible for the structure seen in Figure 5 around $t = 140$ (magnified in the inset) and is the same as the one that produces the structure to the left of the minimum in Figure 4.

In Figure 6 we have left ω_0 constant and varied the damping. Once again our analytic predictions, curves a, b, c (for $\gamma = 5$, 50, 100 respectively in units $\sqrt{(u_0/m)}/b$) do very well with respect to the simulations. Not only do they sit on top of the simulation curves (except for the oscillations) while curves a′, b′, c′ obtained from the $1/v^3$ relation do not, but they also exhibit non-monotonic behavior as γ is varied: curve b is to the left of a but curve c is to the right of b. By contrast, curves a′, b′, c′ exhibit a *monotonic* tendency in that they move leftward in the a′-b′-c′ progression.

5 Concluding remarks

The simple system of a dimer sliding on a periodic substrate offers a testing ground for theoretical approaches aimed at understanding the nature of atomic friction on material substrates. In examining a recently reported nonlinear friction relation [10], we have found, via, our simulations, departures from the prediction of that relation. The departures are interesting, are displayed in Figures 1–3, and can be explained theoretically, as we have shown. Predictions made on the basis of our analysis are borne out excellently by simulations as shown in Figures 5, 6. Our new analytic results are equation (12) for the stopping time of the dimer when thrown over the substrate with an initial velocity, its approximate forms equations (13, 16), and derived expressions such as equations (14, 15). All these results stem from the generalization, equation (12), of the friction relation of reference [10].

Much of the behavior seen in the evolution of the center of mass velocity can be understood physically from the concept of resonance. The bell shape of the resonance given by equation (10) is controlled by damping and the natural frequency of the dimer. Maximum energy is lost in the vibrational motion at and close to resonance. At small values of damping the maximum value of the bell shape is large but the width is narrow so the internal mode does not lose much energy and hence the stopping time is large. Increasing the value of damping brings down the resonance peak but at the same time increases the width of the bell shape. Thus the dimer loses more energy as it spends more time in the resonance region. Large values of damping destroys the width of the resonance curve and again the internal mode is not able to lose much energy; hence the increase in stopping time. The natural frequency determines the position of the peak. Initially, the driving frequency is far away from resonance and not much

energy is being transferred to the internal coordinate. As the center of mass velocity drops down to close to resonance, the transfer of energy reaches a local maximum. However, because the damping is not large the energy cannot be dissipated away immediately and hence is transferred back into translational motion. This back and forth transfer of energy between translational and vibrational motion leads to strong aperiodic oscillations at velocities close to resonance. The nonlinear friction relation given by equation (10) is not able to capture these oscillations. The coupling drives the dimer out of resonance window to where the driving frequency becomes much smaller than the resonant frequency and hence the velocity decays exponentially with time (see Eq. (17)) and the oscillations become periodic. This strong oscillatory behavior can be washed out by increasing the damping of the system due to reasons already mentioned before. Increase in the value of natural frequency shifts the resonance peak to larger values and thus the dimer goes into resonance region at larger driving frequencies.

Our aim in the present paper has been to address some features of atomistic friction. Except for the simplification that the model is confined to a single spatial dimension, it has the necessary ingredients to represent a real dimer or molecule in a controlled microscopic sliding experiment (e.g. [14]) at low temperatures, to the extent that external damping may be considered negligible. Dissipation of translational energy of an object along a surface can occur in two ways, directly and indirectly. Indeed, there has been an ongoing debate in the literature about the relative importance of the source of sliding friction: whether it is electronic or phononic. As explained in detail in the conclusion section of a recent paper by some of the present authors [11] it might make sense to identify background linear friction with electronic, and resonance friction with phononic, sources. For sufficiently large corrugations of the substrate, the latter (the only channel considered in the present paper) can dominate in principle. Nevertheless if the modulation ratio a/b is small, the channel we have considered can be unimportant by comparison, and adlayer velocities relative to the substrate might need to be as high as 30–300 m/s for the resonance friction to be appreciable. Experiments reported so far do not involve such high velocities. Our study has not addressed past observations but targets realizable future scenarios. We hope that in the light of the clear analysis presented in this paper and elsewhere [10], the focus on the resonance friction channel used above will be of help in future observations where that channel may not be overlooked.

It is a pleasure to thank Birk Reichenbach for numerous discussions. This work was supported in part by the NSF under grant INT-0336343.

References

1. M. Urbakh, J. Klafter, D. Gourdon, J. Israelachvili, Nature (London) **430**, 525 (2004)
2. B.N.J. Persson, Phys. Rev. B **48**, 18140 (1993)
3. J. Krim, Surf. Sci **500**, 741 (2002)
4. J.B. Sokoloff, Phys. Rev. B **42**, 760 (1990)
5. A.S. Kovalev, A.I. Landau, Low Temp. Phys. **28**, 423 (2002)
6. O.M. Braun, R. Ferrando, D.E. Tommei, Phys. Rev. E **68**, 051101 (2003)
7. L. Consoli, H.J.F. Knops, A. Fasolino, Phys. Rev. Lett. **85**, 302 (2000)
8. C.M. Mate, G.M. McClelland, R. Erlandsson, S. Chiang, Phys. Rev. Lett. **59**, 1942 (1987)
9. E. Gnecco, R. Bennewitz, T. Gyalog, E. Meyer, J. Phys.: Condens. Matter **13**, R619 (2001)
10. S. Gonçalves, V.M. Kenkre, A.R. Bishop, Phys. Rev. B **70**, 195415 (2004)
11. S. Gonçalves, C. Fusco, A.R. Bishop, V.M. Kenkre, Phys. Rev. B **72**, 195418 (2005)
12. C. Fusco, A. Fasolino, T. Janssen, Eur. Phys J. B **31**, 95 (2003)
13. C. Fusco, A. Fasolino, Thin Solid Films **428**, 34 (2003)
14. A.H. Romero, A.M. Lacasta, J.M. Sancho, Phys. Rev. E **69**, 051105 (2004)
15. O.M. Braun, Phys. Rev. E **63**, 011102 (2001)
16. S.Yu. Krylov, K.B. Jinesh, H. Valk, M. Dienwiebel, J.W.M. Frenken, Phys. Rev. E **71**, 065101(R) (2005)